

Entangled state fusion with Rydberg atoms

Y. Q. Ji^{1,2} · C. M. Dai^{1,2} · X. Q. Shao^{1,2} · X. X. Yi^{1,2,*}

Received: date / Accepted: date

Abstract We propose a scheme for preparation of large-scale entangled GHZ states and W states with neutral Rydberg atoms. The scheme mainly depends on Rydberg antiblockade effect, i.e., as the Rydberg-Rydberg-interaction (RRI) strength and the detuning between the atom transition frequency and the classical laser frequency satisfies some certain conditions, the effective Rabi oscillation between the two ground states and the two excitation Rydberg states would be generated. The prominent advantage is that both two-multiparticle GHZ states and two-multiparticle W states can be fused in this model, especially the success probability for fusion of GHZ states can reach unit. In addition, the imperfections induced by the spontaneous emission is also discussed through numerical simulation.

Keywords Entangled state · fusion · Rydberg atoms

1 Introduction

Due to the promise of applications and rapid experimental progress, the field of quantum information has attracted extensive research. The most advanced experimental demonstrations include trapped ions [1], linear optics [2], superconductors [3,4] and quantum dots in semiconductors [5,6,7]. As a promising candidate for the quantum computer, neutral atom displays another promising approach due to its long-lived encoding of quantum information in atomic hyperfine states and the possibility of manipulating.

*E-mail: yixx@nenu.edu.cn

¹ Center for Quantum Sciences and School of Physics, Northeast Normal University, Changchun, 130024, People's Republic of China

² Center for Advanced Optoelectronic Functional Materials Research, and Key Laboratory for UV Light-Emitting Materials and Technology of Ministry of Education, Northeast Normal University, Changchun 130024, China

When excited to Rydberg state, neutral atom exhibit large dipole moments, which leads to strong and long-range van der Waals or dipole-dipole interactions. The strong and long-range interaction between the excited Rydberg atoms can give rise to the Rydberg blockade that suppress resonant optical excitation of multiple Rydberg atoms [8, 9, 10, 11]. The Rydberg blockade is based on the assumption that one excited atom causes sufficiently large energy shifts of Rydberg states and leads the neighboring atoms away from resonance with laser field and fully blocks its excitation. It is predicted in ref [12] and locally observed in laser cooled atomic systems prepared in magneto-optical traps, both for van der Waals [13, 14, 15] and dipole-dipole interactions [9, 16]. Recently, the phenomenon of Rydberg blockade with two Rydberg atoms located about $4\ \mu m$ [17] and $10\ \mu m$ [18] away, respectively, have been observed in experiments. The Rydberg blockade offers many possibilities for realization of the neutral-atom-based quantum information processing (QIP) tasks [19, 20, 21, 22] and observation of the multiatom effects [23, 24, 25, 26, 27, 28, 29].

When the Rydberg interaction strengths that are too weak to yield the blockade mechanism, yet too strong to be ignored when the atoms are excited with resonant laser fields. The atoms can be excited to the collective Rydberg states [8]. In addition, when the detuning between the atom transition frequency and the frequency of a classical laser satisfies some conditions with Rydberg interaction strength, the atoms also can be excited to the collective Rydberg states. Hence, the Rydberg antiblockade regime can be generated. This case has theoretically been studied and used for preparation of entanglement and logic gate [30, 31, 32, 33, 34, 35, 36].

As two of the most basic entangled states, the Greenberger-Horne-Zeilinger (*GHZ*) states [37] and the *W* states [38, 39] show great advantage and play an important role in QIP. These two kinds of entangled states can perform different tasks of quantum information theory [40, 41, 42]. Therefore, the preparation of entangled state is particularly important. However, it is difficult to create multipartite entangled states in a realistic situation because the dynamics becomes more complex as the number of particles increases. Thus simple and efficient schemes to prepare large-scale multipartite entangled states are very important. In recent works, quantum state fusion has been put forward to realize large-size multipartite entangled states [43, 44, 45, 46, 47], i.e., one can get a larger entangled state from two entangled states on the condition that one qubit of each entangled states is sent to the fusion operation. Such as, Özdemir *et al.* used a simple optical fusion gate to get an $(m+n-2)$ -qubit *W* states from an m -qubit *W* states and an n -qubit *W* states [43]. Nevertheless, most schemes are just for fusion *W* states.

In this paper, we consider the implementation of entangled states fusion with Rydberg atoms confined in spatially separated dipole traps subject to the Rydberg antiblockade effect. We derive the effective Hamiltonian of a two-atoms computational subspace and show how to tailor it in order to implement the specific evolution. Then entangled states fusion with Rydberg atoms can be implemented using this specific evolution. Our scheme has the following characteristics: (1) Adopting neutral atoms as qubits, the quantum information

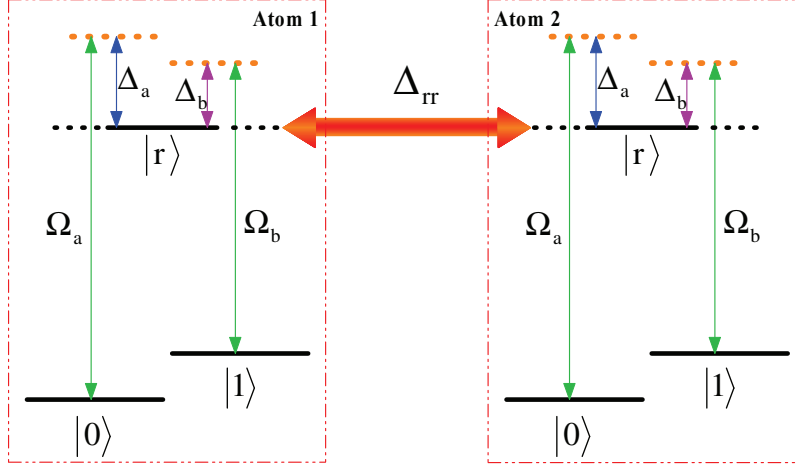


Fig. 1 Schematic view of atomic-level configuration. $|r\rangle$ is the Rydberg state, while $|0\rangle$ and $|1\rangle$ are two ground states. Δ_{rr} denotes the RRI strength. The atomic transition $|0\rangle \leftrightarrow |r\rangle$ are driven by a classical laser field with the Rabi frequency Ω_a and the transition $|1\rangle \leftrightarrow |r\rangle$ are driven by a classical laser field with the Rabi frequency Ω_b . $\Delta_{a(b)}$ represents the corresponding detuning parameter.

is encoded into the stable hyperfine ground states and distant atoms interact with each other through the RRI. (2) Only one RRI term is produced and thus the asymmetric Rydberg coupling strengths are avoided. (3) Not only two multiparticle W states can be fused but also two multiparticle GHZ states can be fused in this model, especially the success probability for fusion of GHZ states can reach unit.

The rest of the paper is organized as follows. In Sec. 2, we derive the effective Hamilton of two Rydberg. In Sec. 3 and Sec. 4, we describe how to fuse two multiparticle GHZ states and multiparticle W states, respectively. In Sec. 5, a discussion is given. At last, a summary is given in Sec. 6.

2 Basic model

We consider two identical ^{87}Rb atoms individually trapped in two tightly focused optical tweezers [48, 49], with a typical separation of 5-10 microns, and the relevant configuration of atomic level is illustrated in Fig 1, each one has two ground states $|0\rangle$ and $|1\rangle$ and a Rydberg state $|r\rangle$, where $|0\rangle$ and $|1\rangle$ corresponds to atomic levels $|F = 1, M = 1\rangle$ and $|F = 2, M = 2\rangle$ of $5S_{1/2}$ manifold, and the Rydberg state $|r\rangle = |F = 3, M = 3\rangle$ of $58D_{3/2}$ directly coupled to the ground states by a single exciting laser. The transition $|0(1)\rangle \leftrightarrow |r\rangle$ is then driven by a nonresonant classical laser field with Rabi frequencies $\Omega_{a(b)}$, frequency $\omega_{a(b)}$, and detuning $\Delta_{a(b)}$. As is well known, Rydberg atoms exhibit huge dipole moments which lead to large dipole-dipole interactions. We shall assume that the dipole-dipole interaction manifests it-

self only when both of atoms are in their Rydberg states. In other words, we assume $\hat{U}_{rr} = \Delta_{rr}|rr\rangle\langle rr|$ and Δ_{rr} is the RRI strength which mainly depends on the principal quantum numbers of the Rydberg atoms and the distance between the Rydberg atoms. Thus, the Hamiltonian of the whole system can be written as

$$\hat{H} = \hat{H}_1 \otimes \hat{I}_2 + \hat{I}_1 \otimes \hat{H}_2 + \hat{U}_{rr}, \quad (1)$$

with

$$\begin{aligned} \hat{H}_p = & \frac{\Omega_a}{2} e^{i\omega_a t} |0\rangle_p \langle r| + \frac{\Omega_b}{2} e^{i\omega_b t} |1\rangle_p \langle r| + \text{H.c.} \\ & + \sum_{j=0,1,r} \omega_j |j\rangle_p \langle j|, \end{aligned} \quad (2)$$

\hat{I}_p denotes the 3×3 identity matrix ($p = 1, 2$). After moving \hat{H} to the interaction picture with respect to Hamiltonian $\sum_{p=1,2} \sum_{j=0,1,r} \omega_j |j\rangle_p \langle j|$, we can get

$$\hat{H}'_p = \frac{\Omega_a}{2} e^{i\Delta_a t} |0\rangle_p \langle r| + \frac{\Omega_b}{2} e^{i\Delta_b t} |1\rangle_p \langle r| + \text{H.c.}, \quad (3)$$

and \hat{U}_{rr} remains unchanged. To see clearly the role of the RRI term, we rewrite the full Hamiltonian with the basis $\{|00\rangle, |01\rangle, |0r\rangle, |10\rangle, |11\rangle, |1r\rangle, |r0\rangle, |r1\rangle, |rr\rangle\}$ and move to the rotation frame with respect to \hat{U}_{rr} . Thus, the full Hamiltonian is transformed to

$$\begin{aligned} \hat{H}'' = & \frac{\Omega_a}{2} e^{i\Delta_a t} (|00\rangle\langle r0| + |10\rangle\langle rb| + |00\rangle\langle 0r| + |01\rangle\langle 1r|) \\ & + \frac{\Omega_a}{2} e^{i(\Delta_a - \Delta_{rr})t} (|r0\rangle\langle rr| + |0r\rangle\langle rr|) \\ & + \frac{\Omega_b}{2} e^{i\Delta_b t} (|01\rangle\langle r0| + |11\rangle\langle r1| + |10\rangle\langle 0r| + |11\rangle\langle 1r|) \\ & + \frac{\Omega_b}{2} e^{i(\Delta_b - \Delta_{rr})t} (|r1\rangle\langle rr| + |1r\rangle\langle rr|) + \text{H.c.} \end{aligned} \quad (4)$$

In the following, we assume $\Omega_a = \Omega_b = \Omega$ and $\Delta_a = \Delta_b = \Delta$, $\Delta_a = \omega_a - (\omega_r - \omega_0)$ and $\Delta_b = \omega_b - (\omega_r - \omega_1)$. Note that, whether ω_0 and ω_1 are equal depend on ω_a and ω_b . In fact, ω_a and ω_b are not equal. So the states $|0\rangle$ and $|1\rangle$ are not degenerate. To achieve the antiblockade regime, we here adjust the classical field and RRI strength to make the parameters satisfy $2\Delta = \Delta_{rr}$. Then, the large detuned condition $\Delta \gg \Omega/2$ would induce the effective Hamiltonian [50]

$$\begin{aligned} \hat{H}_e = & \frac{\Omega^2}{2\Delta} [(|00\rangle + |rr\rangle)(\langle 00| + \langle rr|) + (|11\rangle + |rr\rangle)(\langle 11| + \langle rr|)] \\ & - \frac{\Omega^2}{2\Delta} [(|0r\rangle + |1r\rangle)(\langle 0r| + \langle 1r|) + (|r0\rangle + |r1\rangle)(\langle r0| + \langle r1|)] \\ & + \frac{\Omega^2}{4\Delta} [(|00\rangle + |11\rangle)(\langle 10| + \langle 01|) + (|01\rangle + |10\rangle)(\langle 00| + \langle 11|)] \\ & - \frac{\Omega^2}{4\Delta} [(|0r\rangle + |1r\rangle)(\langle r0| + \langle r1|) + (|r0\rangle + |r1\rangle)(\langle 0r| + \langle 1r|)] \\ & - \frac{\Omega^2}{2\Delta} [|0r\rangle\langle r0| + |1r\rangle\langle r1| + |r0\rangle\langle 0r| + |r1\rangle\langle 1r|] \end{aligned}$$

$$\begin{aligned}
& + \frac{\Omega^2}{2\Delta} [(|01\rangle + |10\rangle)\langle rr| + |rr\rangle(\langle 01| + \langle 10|)] \\
& + \frac{\Omega^2}{2\Delta} (|01\rangle\langle 10| + |10\rangle\langle 01|).
\end{aligned} \tag{5}$$

Because the initial state is among the basis $\{|00\rangle, |01\rangle, |10\rangle, |11\rangle\}$, the states $|0r\rangle, |r0\rangle, |1r\rangle$ and $|r1\rangle$ have no energy exchange with the other states, after we reject these states, the Eq. (5) becomes

$$\begin{aligned}
\hat{H}_{\text{eff}} = & \frac{\Omega^2}{2\Delta} [(|00\rangle + |rr\rangle)(\langle 00| + \langle rr|) + (|11\rangle + |rr\rangle)(\langle 11| + \langle rr|)] \\
& + \frac{\Omega^2}{4\Delta} [(|00\rangle + |11\rangle)(\langle 01| + \langle 10|) + (|01\rangle + |10\rangle)(\langle 00| + \langle 11|)] \\
& + \frac{\Omega^2}{2\Delta} [(|01\rangle + |10\rangle)\langle rr| + |rr\rangle(\langle 01| + \langle 10|)] \\
& + \frac{\Omega^2}{2\Delta} (|01\rangle\langle 10| + |10\rangle\langle 01|).
\end{aligned} \tag{6}$$

From Eq. (6) we can see that the effective Rabi oscillation between the two ground states and the two excited Rydberg states are generated, which is out of the Rydberg blockade regime.

For the initial states $|00\rangle, |01\rangle, |10\rangle$ and $|11\rangle$, the roles of the effective evolution operator $e^{-i\hat{H}_{\text{eff}}t}$ can be illustrated as follows:

$$\begin{aligned}
|00\rangle & \rightarrow a|00\rangle + b|01\rangle + b|10\rangle + c|11\rangle + d|rr\rangle \\
|01\rangle & \rightarrow b|00\rangle + a|01\rangle + c|10\rangle + b|11\rangle + d|rr\rangle \\
|10\rangle & \rightarrow b|00\rangle + c|01\rangle + a|10\rangle + b|11\rangle + d|rr\rangle \\
|11\rangle & \rightarrow c|00\rangle + b|01\rangle + b|10\rangle + a|11\rangle + d|rr\rangle,
\end{aligned} \tag{7}$$

with

$$\begin{aligned}
a & = \frac{1}{8} \left(3 + 4e^{-i\frac{\Omega^2 t}{2\Delta}} + e^{-i\frac{2\Omega^2 t}{\Delta}} \right) \\
b & = \frac{1}{8} \left(-1 + e^{-i\frac{2\Omega^2 t}{\Delta}} \right) \\
c & = \frac{1}{8} \left(3 - 4e^{-i\frac{\Omega^2 t}{2\Delta}} + e^{-i\frac{2\Omega^2 t}{\Delta}} \right) \\
d & = \frac{1}{4} \left(-1 + e^{-i\frac{2\Omega^2 t}{\Delta}} \right).
\end{aligned} \tag{8}$$

After choosing the parameters satisfy $\Omega^2 t / \Delta = \pi$, Eq. (7) can be simplified to

$$\begin{aligned}
|00\rangle & \rightarrow \frac{1}{\sqrt{2}} (|00\rangle + i|11\rangle) \\
|01\rangle & \rightarrow \frac{1}{\sqrt{2}} (|01\rangle + i|10\rangle) \\
|10\rangle & \rightarrow \frac{1}{\sqrt{2}} (|10\rangle + i|01\rangle) \\
|11\rangle & \rightarrow \frac{1}{\sqrt{2}} (|11\rangle + i|00\rangle),
\end{aligned} \tag{9}$$

in this process, we ignore the global phase factor $e^{-i\frac{\pi}{4}}$.

For the result of Eq. (9), one can find some interesting things, such as preparation of entangle states, i.e., the entanglement between $|00\rangle$ and $|11\rangle$ or $|01\rangle$ and $|10\rangle$.

3 Fusing atomic GHZ states

Now, we introduce how to implement an $(m+n-2)$ -qubit GHZ states fusion scheme from an m -qubits GHZ states and an n -qubits GHZ states based on Rydberg atoms, where $m \geq 3$ and $n \geq 3$. The entangled GHZ states of Alice and Bob are

$$\begin{aligned} |GHZ_m\rangle_A &= \frac{1}{\sqrt{2}} (|(m-1)_0\rangle|1_0\rangle + |(m-1)_1\rangle|1_1\rangle), \\ |GHZ_n\rangle_B &= \frac{1}{\sqrt{2}} (|(n-1)_0\rangle|1_0\rangle + |(n-1)_1\rangle|1_1\rangle). \end{aligned} \quad (10)$$

Here $|(m-1)_0\rangle$ denotes the $(m-1)$ atoms remain $|0\rangle$. To start the fusion process, the two atoms, respectively, belong to Alice and Bob, will be sent into the third party Claire who receives two atoms with Rydberg antiblockade effect to merge and inform them when the task is successful. So the initial state of the whole system is

$$|\psi_0\rangle = |GHZ_m\rangle_A \otimes |GHZ_n\rangle_B. \quad (11)$$

The far-off-resonant interaction between the classical laser field and the two atoms will lead the initial states evolve to the following state (according the result in Eq. (7))

$$\begin{aligned} |\psi_1\rangle &= \frac{1}{2} |(m-1)_0\rangle |(n-1)_0\rangle \frac{1}{\sqrt{2}} (|00\rangle + i|11\rangle) \\ &+ \frac{1}{2} |(m-1)_0\rangle |(n-1)_1\rangle \frac{1}{\sqrt{2}} (|01\rangle + i|10\rangle) \\ &+ \frac{1}{2} |(m-1)_1\rangle |(n-1)_0\rangle \frac{1}{\sqrt{2}} (|10\rangle + i|01\rangle) \\ &+ \frac{1}{2} |(m-1)_1\rangle |(n-1)_1\rangle \frac{1}{\sqrt{2}} (|11\rangle + i|00\rangle). \end{aligned} \quad (12)$$

Then the two atoms will be detected by Claire. There are four possible detection results for the fusion mechanism. If the detection result is $|00\rangle$, the remaining atoms are in the following state

$$|\psi_2\rangle = \frac{1}{\sqrt{2}} (|(m-1)_0\rangle |(n-1)_0\rangle + i|(m-1)_1\rangle |(n-1)_1\rangle). \quad (13)$$

There are only relative phase differences between the state $|\psi_2\rangle$ and the standard GHZ states. After Alice or Bob performs the one-qubit phase gate on one of the atoms that she or he has, i.e., $\{|0\rangle \rightarrow |0\rangle, |1\rangle \rightarrow i|1\rangle\}$, the state in Eq. (13) will become an $m+n-2$ -qubit GHZ states and the corresponding success probability is $1/4$.

If the detection result is $|11\rangle$, the systemic state will collapse to

$$|\psi_3\rangle = \frac{1}{\sqrt{2}} (i|(m-1)_0\rangle |(n-1)_0\rangle + |(m-1)_1\rangle |(n-1)_1\rangle), \quad (14)$$

similarly, we also can obtain an $(m+n-2)$ -qubit GHZ states if Alice or Bob performs similar operation.

If the detection result is $|01\rangle$ or $|10\rangle$, the systemic state will collapse to

$$|\psi_4\rangle = \frac{1}{\sqrt{2}}(|(m-1)_0\rangle|(n-1)_1\rangle + i|(m-1)_1\rangle|(n-1)_0\rangle) \quad (15)$$

or

$$|\psi_5\rangle = \frac{1}{\sqrt{2}}(i|(m-1)_0\rangle|(n-1)_1\rangle + |(m-1)_1\rangle|(n-1)_0\rangle), \quad (16)$$

respectively. Also the states in Eqs (15,16) can be transformed into a standard GHZ states by one-qubit phase gate on any one of the $(m+n-2)$ atoms. Hence, the total success probability for fusion an m -qubit GHZ states and an n -qubit GHZ state can reach unit.

4 Fusing atomic W states

Now, we introduce how to implement an $(m+n-2)$ -qubit atomic W states fusion scheme. The atomic entangled W states of Alice and Bob are

$$\begin{aligned} |W_m\rangle_A &= \frac{1}{\sqrt{m}}(|(m-1)_0\rangle|1_1\rangle + \sqrt{m-1}|W_{m-1}\rangle|1_0\rangle), \\ |W_n\rangle_B &= \frac{1}{\sqrt{n}}(|(n-1)_0\rangle|1_1\rangle + \sqrt{n-1}|W_{n-1}\rangle|1_0\rangle). \end{aligned} \quad (17)$$

To start the fusion process, the two atoms (atom1 and atom 2) will be sent into the third party Claire. So the initial state of the whole system is

$$|\phi_0\rangle = |W_m\rangle_A \otimes |W_n\rangle_B. \quad (18)$$

The far-off-resonant interaction between the classical laser field and the two atoms will lead the initial states evolve to the following state

$$\begin{aligned} |\phi_1\rangle &= \frac{1}{\sqrt{mn}}|(m-1)_0\rangle|(n-1)_0\rangle \otimes \frac{1}{\sqrt{2}}(|11\rangle + i|00\rangle) \\ &\quad + \frac{\sqrt{(m-1)(n-1)}}{\sqrt{mn}}|W_{m-1}\rangle|W_{n-1}\rangle \otimes \frac{1}{\sqrt{2}}(|00\rangle + i|11\rangle) \\ &\quad + \frac{\sqrt{n-1}}{\sqrt{mn}}|(m-1)_0\rangle|W_{n-1}\rangle \otimes \frac{1}{\sqrt{2}}(|10\rangle + i|01\rangle) \\ &\quad + \frac{\sqrt{m-1}}{\sqrt{mn}}|W_{m-1}\rangle|(n-1)_0\rangle \otimes \frac{1}{\sqrt{2}}(|01\rangle + i|10\rangle). \end{aligned} \quad (19)$$

Then Claire will detect the states of two atoms and inform Alice and Bob whether the task is successful. There are four possible detection results from Eq. (19). If the detection result is $|10\rangle$, the remaining atoms are in the following state

$$|\phi_2\rangle = \frac{1}{\sqrt{2mn}}(\sqrt{n-1}|(m-1)_0\rangle|W_{n-1}\rangle + \sqrt{m-1}|W_{m-1}\rangle|(n-1)_0\rangle). \quad (20)$$

After Bob performs the one-qubit phase gate on all the atoms that he has, i.e., $\{|0\rangle \rightarrow |0\rangle, |1\rangle \rightarrow i|1\rangle\}$, the state in Eqs. (20) will become

$$\begin{aligned} |\phi'_2\rangle &= \frac{1}{\sqrt{2mn}} (\sqrt{n-1}|(m-1)_0\rangle|W_{n-1}\rangle + \sqrt{m-1}|W_{m-1}\rangle|(n-1)_0\rangle) \\ &= \frac{\sqrt{n+m-2}}{\sqrt{2mn}} |W_{n+m-2}\rangle, \end{aligned} \quad (21)$$

where we have ignored the global phase factor i and used $\sqrt{k}|W_k\rangle = \sqrt{i}|W_i\rangle|(k-i)_{g_0}\rangle + \sqrt{i-1}|i_{g_0}\rangle|W_{k-i}\rangle$. Obviously, $|\phi'_2\rangle$ is a standard atomic W states, i.e., $|W_{n+m-2}\rangle$, and the success probability obtaining the $|\phi'_2\rangle$ state is $(n+m-2)/(2mn)$.

If the detection result is $|01\rangle$, the systemic state becomes

$$|\phi_3\rangle = \frac{1}{\sqrt{2mn}} (i\sqrt{n-1}|(m-1)_0\rangle|W_{n-1}\rangle + \sqrt{m-1}|W_{m-1}\rangle|(n-1)_0\rangle). \quad (22)$$

After Alice performs the one-qubit phase gate on all the atoms that she has, the state in Eq. (22) will become Eq. (21), and the success probability is $(n+m-2)/(2mn)$. However, the cases of $|00\rangle$ and $|11\rangle$ are failure. Thus the total success probability for the fusion process is

$$P_{n+m-2} = \frac{n+m-2}{mn}. \quad (23)$$

5 Discussion

In the above, the dissipation has not been taken into account. Thus, we investigate the influence of spontaneous emission on this method. When decoherence effects are taken into account and under the assumptions that the decay channels are independent, the master equation of the whole system can be expressed by the Lindblad form [51,52]

$$\dot{\rho} = -i[H, \rho] - \frac{1}{2} \sum_{k=1}^4 \left[\hat{\mathcal{L}}_k^\dagger \hat{\mathcal{L}}_k \rho - 2\hat{\mathcal{L}}_k \rho \hat{\mathcal{L}}_k^\dagger + \rho \hat{\mathcal{L}}_k^\dagger \hat{\mathcal{L}}_k \right], \quad (24)$$

where ρ is the density matrix of the whole system and γ denotes the spontaneous emission rate, $\hat{\mathcal{L}}_1 = \sqrt{\gamma/2}|0\rangle_1\langle r|$, $\hat{\mathcal{L}}_2 = \sqrt{\gamma/2}|1\rangle_1\langle r|$, $\hat{\mathcal{L}}_3 = \sqrt{\gamma/2}|0\rangle_2\langle r|$ and $\hat{\mathcal{L}}_4 = \sqrt{\gamma/2}|1\rangle_2\langle r|$ are Lindblad operators that describe the dissipative processes. For simplicity, here we have assumed the Rydberg state $|r\rangle$ has an equal spontaneous emission rate for the two ground states $|0\rangle$ and $|1\rangle$.

To check the performance, the fidelity is defined as $\langle \psi_{ideal} | \hat{\rho}(t) | \psi_{ideal} \rangle$. In Fig. 2, we choose $|00\rangle$ act as initial state and $\frac{1}{\sqrt{2}}(|00\rangle + i|11\rangle)$ act as final state. One can see that the curves plotted with the full Hamiltonian (without γ) and effective Hamiltonian (without γ), respectively, fit well with each other, which proves the effective Hamiltonian is valid in this paper. In Fig. 3, we use the initial state $|00\rangle$ corresponding final state $\frac{1}{\sqrt{2}}(|00\rangle + i|11\rangle)$ to check the performance. From Fig. 3, we can see that the fidelity is very high at the

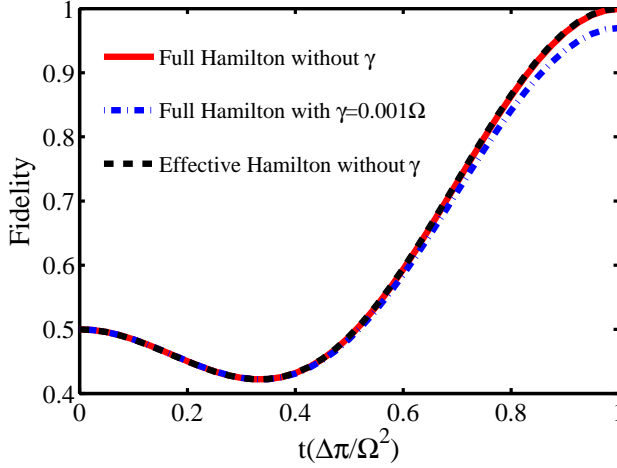


Fig. 2 Choosing the initial state $|00\rangle$ and final state $\frac{1}{\sqrt{2}}(|00\rangle + i|11\rangle)$ at the time interval $t \in [0, \Delta\pi/\Omega^2]$ to check the performance. The red solid line and black dashed line, respectively, denotes the fidelity with the full Hamilton and effective Hamilton with out spontaneous emission γ . The blue dot-dashed line denotes the fidelity with the full Hamilton with $\gamma = 0.001\Omega$. The other parameters are chosen as $\Omega_a = \Omega_b = \Omega = 1$, $\Delta_a = \Delta_b = \Delta = 40$, $\Delta_{rr} = 2\Delta = 80$.

optimal time and the spontaneous emission lead to the fidelity decrease. For the initial states $|01\rangle$, $|10\rangle$ and $|11\rangle$, decoherence effects is the same to each other, this is because the evolution of $|00\rangle$ to $\frac{1}{\sqrt{2}}(|00\rangle + i|11\rangle)$ must through the intermediate state $|rr\rangle$, the states $|0r\rangle$, $|r0\rangle$, $|1r\rangle$ and $|r1\rangle$ are not exist due to the large detuning. From another perspective, if we change $|0\rangle$ to $|1\rangle$ or $|1\rangle$ to $|0\rangle$ on each of two atoms, the effective Hamilton remain unchanged. Therefore, the decoherence effects for four final states are considered the same.

For the GHZ states fusion, due to the fidelity of the states $\frac{1}{\sqrt{2}}(|00\rangle + i|11\rangle)$, $\frac{1}{\sqrt{2}}(|01\rangle + i|10\rangle)$, $\frac{1}{\sqrt{2}}(|10\rangle + i|01\rangle)$ and $\frac{1}{\sqrt{2}}(|11\rangle + i|00\rangle)$ are considered equal to each other, so we assume it equal to F' . Hence, the final fidelity (Eq. (12) as final state) can be represented as $F_{GHZ} = \frac{1}{2}F' + \frac{1}{2}F' + \frac{1}{2}F' + \frac{1}{2}F' = F'$. However, for the W states fusion, the final fidelity (Eq. (19) as final state) can be represented as $F_W = \frac{1}{mn}F' + \frac{(m-1)(n-1)}{mn}F' + \frac{n-1}{mn}F' + \frac{m-1}{mn}F' = F'$. In the fusion process, single-qubit gates imperfections can be quite small, leading to fidelity errors $O(10^{-4})$ [32]. Hence, we have ignored the influence of one-qubit phase gate in this schemes, i.e., $F_{GHZ} = F_W \simeq F'$. The robustness against operational imperfection is also a main factor for the feasibility of the schemes. In the above numerical simulations, for simplicity we only consider the case $\Omega_a = \Omega_b = \Omega$. So a numerical simulation is performed to check the fidelity by varying error parameters of the mismatch among the Rabi frequency of classical laser field and the interaction time through solving the master equation numerically with the full Hamiltonian. We define $\delta\Omega = \frac{\Omega_a - \Omega_b}{\Omega_b}$ and

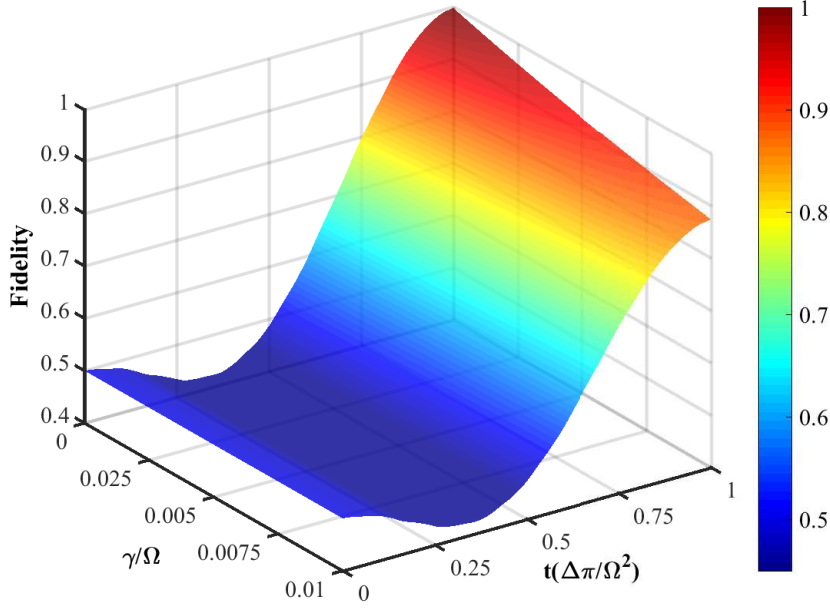


Fig. 3 The effect of decoherence induced by spontaneous emission of Rydberg state as well as evolution time t for the evolution of initial states $|00\rangle$. The parameters are chosen as $\Omega_a = \Omega_b = \Omega = 1$, $\Delta_a = \Delta_b = \Delta = 40$, $\Delta_{rr} = 2\Delta = 80$.

$\delta t = \frac{t}{t_0}$, t_0 is the optimal evolution time. The fidelity varies the variations in different parameters are shown in Fig. 4 and Fig. 5. In Fig. 4, we plot the fidelity with respect to γ/Ω_b as well as $\delta\Omega$ at the optimal time $\frac{\Delta\pi}{\Omega^2}$, where we have set $\Omega_b = 1$, $\Delta_a = \Delta_b = \Delta = 40$, $\Delta_{rr} = 2\Delta = 80$. In Fig. 5, we plot the fidelity with respect to δt as well as $\delta\Omega$ when $\Omega_b = 1$, $\Delta_a = \Delta_b = \Delta = 40$, $\Delta_{rr} = 2\Delta = 80$ and $\gamma = 0$. As shown in the figures, the schemes is a little sensitive to the variation in the laser Rabi frequency and the interaction time. But that is not a serious problem to realize the schemes because the laser Rabi frequency and the interaction time can be precisely controlled in experiment.

In Ref. [48,49], the parameters are chosen as follows: RRI strength $\Delta_{rr} \simeq 2 \times 10^3$ MHz, Rydberg state decay rate $\gamma = 10$ kHz, it is reasonable if we set $\Delta_a = \Delta_b = 10^3$ MHz, and $\Omega_a = \Omega_b = 50$ MHz. By substituting these values into the master equation, the fidelities $F' = 99.4\%$ for fusion of GHZ states and W states could be achieved.

6 Summary

In summary, we have proposed a method to fuse entangled GHZ states and W states based on neutral Rydberg atoms. This scheme works well in the regime

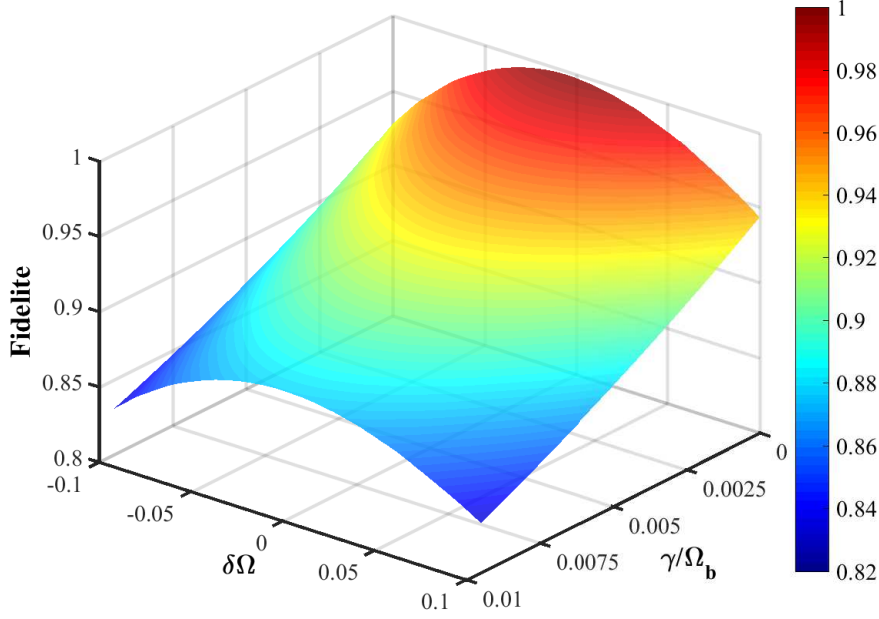


Fig. 4 Fidelity with respect to γ/Ω_b as well as $\delta\Omega$ ($\delta\Omega = \frac{\Omega_a - \Omega_b}{\Omega_b}$) at the optimal time $\frac{\Delta\pi}{\Omega^2}$. The other parameters are chosen as $\Omega_b = 1$, $\Delta_a = \Delta_b = \Delta = 40$, $\Delta_{rr} = 2\Delta = 80$.

where the Rydberg interaction holds a comparable strength to the detuning. Final numerical simulation based on one group of experiment parameters shows that our scheme could be feasible under current technology and have a high fidelity. We believe our work will be useful for the experimental realization of quantum information with neutral atoms in the near future.

ACKNOWLEDGMENTS

This work is supported by National Natural Science Foundation of China (NSFC) under Grants No. 11534002, No. 61475033 and Fundamental Research Funds for the Central Universities under Grant No. 2412016KJ004.

References

1. Blatt, R., Wineland, D.: Entangled states of trapped atomic ions. *Nature (London)* **453**, 1008 (2008)
2. Kok, P., Munro, W.J., Nemoto, K., Ralph, T.C., Dowling, J.P., Milburn, G.J.: Linear optical quantum computing with photonic qubits. *Rev. Mod. Phys.* **79**, 135 (2007)
3. Clarke, J., Wilhelm, F.K.: Superconducting quantum bits. *Nature (London)* **453**, 1031 (2008)

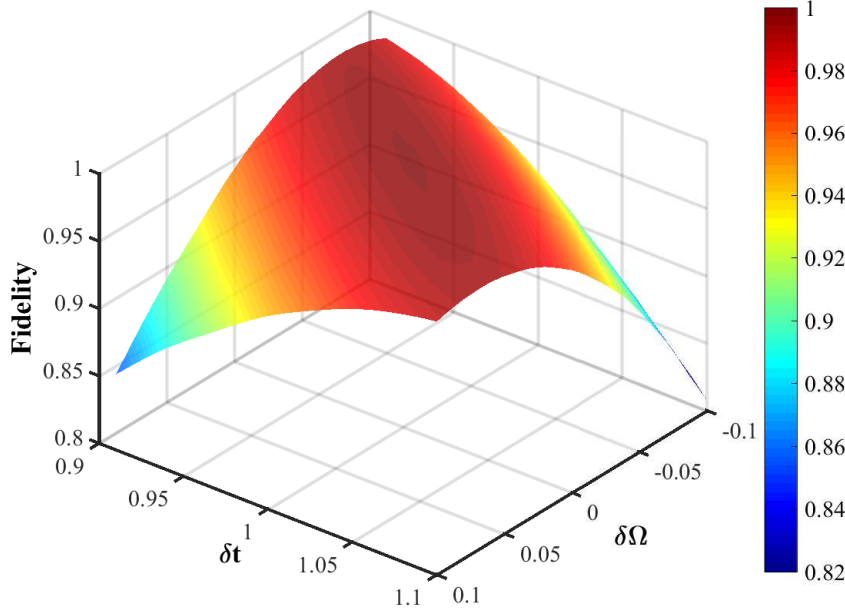


Fig. 5 Fidelity with respect to δt as well as $\delta\Omega$, where $\delta t = \frac{t}{t_0}$, and $\delta\Omega = \frac{\Omega_a - \Omega_b}{\Omega_b}$, t is actual time of evolution and t_0 is the optimal evolution time. The other parameters are chosen as $\Omega_b = 1$, $\Delta_a = \Delta_b = \Delta = 40$, $\Delta_{rr} = 2\Delta = 80$ and $\gamma = 0$.

4. DiCarlo, L., Chow, J.M., Gambetta, J.M., Bishop, L.S., Schuster, D.I., Majer, J., Blais, A., Frunzio, L., Girvin, S.M., Schoelkopf, R.J.: Demonstration of two-qubit algorithms with a superconducting quantum processor. *Nature (London)* **460**, 240 (2009)
5. Petta, J.R., Gossard, A.C.: Coherent manipulation of coupled electron spins in semiconductor quantum dots. *Science* **309**, 2180 (2005)
6. Li, X., Wu, Y., Steel, D., Gammon, D., Stievater, T.H., Katzer, D.S., Park, D., Piermarocchi, C., Sham, L.J.: An all-optical quantum gate in a semiconductor quantum dot. *Science* **301**, 809 (2003)
7. Barthel, C., Reilly, D.J., Marcus, C.M., Hanson, M.P., Gossard, A.C.: Rapid single-shot measurement of a singlet-triplet qubit. *Phys. Rev. Lett.* **103**, 160503 (2009)
8. Jaksch, D., Cirac, J.I., Zoller, P., Rolston, S.L., Côté, R., Lukin, M.D.: Fast quantum gates for neutral atoms. *Phys. Rev. Lett.* **85**, 2208 (2000)
9. Vogt, T., Viteau, M., Zhao, J., Chotia, A., Comparat, D., Pillet, P.: Dipole blockade at Förster resonances in high resolution laser excitation of Rydberg states of cesium atoms. *Phys. Rev. Lett.* **97**, 083003 (2006)
10. Honer, J., Low, R., Weimer, H., Pfau, T., Buchler, H.P.: Artificial atoms can do more than atoms: Deterministic single photon subtraction from arbitrary light fields. *Phys. Rev. Lett.* **107**, 093601 (2011)
11. Dudin, Y.O., Li, L., Bariani, F., Kuzmich, A.: Observation of coherent many-body Rabi oscillations. *Nat. Phys.* **8**, 790 (2012)
12. Lukin, M.D., Fleischhauer, M., Cote, R., Duan, L.M., Jaksch, D., Cirac, J.I., Zoller, P.: Dipole blockade and quantum information processing in mesoscopic atomic ensembles. *Phys. Rev. Lett.* **87**, 037901 (2001)

13. Tong, D., Farooqi, S.M., Stanojevic, J., Krishnan, S., Zhang, Y.P., Côté, R., Eyler, E.E., Gould, P.L.: Local blockade of Rydberg excitation in an ultracold gas. *Phys. Rev. Lett.* **93**, 063001 (2004)
14. Cubel, L.T., Reinhard, A., Berman, P.R., Raithel, G.: Spatial control of recollision wave packets with attosecond precision. *Phys. Rev. Lett.* **95**, 253001 (2005)
15. Singer, K., Lamour, M.R., Amthor, T., Marcassa, L.G., Weidemüller, M.: Suppression of excitation and spectral broadening induced by interactions in a cold gas of Rydberg atoms. *Phys. Rev. Lett.* **93**, 163001 (2004)
16. Anderson, W., Veale, J., Gallagher, T.: Resonant dipole-dipole energy transfer in a nearly frozen Rydberg gas. *Phys. Rev. Lett.* **80**, 249 (1998)
17. Gaëtan, A., Miroshnychenko, Y., Wilk, T., Chotia, A., Viteau, M., Comparat, D., Pillet, P., Browaeys, A., Grangier, P.: Observation of collective excitation of two individual atoms in the Rydberg blockade regime. *Nat. Phys.* **5**, 115 (2009)
18. Urban, E., Johnson, T.A., Henage, T., Isenhower, L., Yavuz, D.D., Walker, T.G., Saffman, M.: Observation of Rydberg blockade between two atoms. *Nat. Phys.* **5**, 110 (2009)
19. Saffman, M., Mølmer, K.: Efficient multiparticle entanglement via asymmetric Rydberg blockade. *Phys. Rev. Lett.* **102**, 240502 (2009)
20. Saffman, M., Walker, T.G., Mølmer, K.: Quantum information with Rydberg atoms. *Rev. Mod. Phys.* **82**, 2313 (2010)
21. Yang, R.C., Lin, X., Ye, L.X., Chen, X., He, J., Liu, H.Y.: Generation of singlet states with rydberg blockade mechanism and driven by adiabatic passage. *Quantum Inf. Process.* **15**, 731 (2016)
22. Khazali, M., Lau, H.W., Humeniuk, A., Simon, C.: Large energy superpositions via rydberg dressing. *Phys. Rev. A*, **94** 023408 (2016)
23. Schachenmayer, J., Lesanovsky, I., Micheli, A., Daley, A.J.: Dynamical crystal creation with polar molecules or Rydberg atoms in optical lattices. *New J. Phys.* **12**, 103044 (2010)
24. Schwarzkopf, A., Sapiro, R.E., Raithel, G.: Imaging spatial correlations of Rydberg excitations in cold atom clouds. *Phys. Rev. Lett.* **107**, 103001 (2010)
25. van Bijnen, R.M.W., Smit, S., van Leeuwen, K.A.H., Vredenburg, E.J.D., Kokkelmans, S.J.J.M.F.: Adiabatic formation of Rydberg crystals with chirped laser pulses. *J. Phys. B* **44**, 184008 (2011)
26. Viteau, M., Bason, M.G., Radogostowicz, J., Malossi, N., Ciampini, D., Morsch, O., Arimondo, E.: Rydberg excitations in Bose-Einstein condensates in quasi-one-dimensional potentials and optical lattices. *Phys. Rev. Lett.* **107**, 060402 (2011)
27. Lesanovsky, I.: Liquid ground state, gap, and excited states of a strongly correlated spin chain. *Phys. Rev. Lett.* **108**, 105301 (2011)
28. Schauf, P., Cheneau, M., Endres, M., Fukuhara, T., Hild, S., Omran, A., Pohl, T., Gross, C., Kuhr, S., Bloch, I.: Observation of spatially ordered structures in a two-dimensional Rydberg gas. *Nature (London)* **491**, 87 (2012)
29. Petrosyan, D., Molmer, K.: Stimulated adiabatic passage in a dissipative ensemble of atoms with strong Rydberg-state interactions. *Phys. Rev. A* **87**, 033416 (2013)
30. Müller, M., Lesanovsky, I., Weimer, H., Böhler, H.P., Zoller, P.: Mesoscopic rydberg gate based on electromagnetically induced transparency. *Phys. Rev. Lett.* **102**, 170502 (2009)
31. Carr, A.W., Saffman, M.: Preparation of entangled and antiferromagnetic states by dissipative Rydberg pumping. *Phys. Rev. Lett.* **111**, 033607 (2013)
32. Shao, X.Q., You, J.B., Zheng, T.Y., Oh, C.H., Zhang, S.: Stationary three-dimensional entanglement via dissipative Rydberg pumping. *Phys. Rev. A* **89**, 052313 (2014)
33. Su, S.L., Guo, Q., Wang, H.F., Zhang, S.: Simplified scheme for entanglement preparation with Rydberg pumping via dissipation. *Phys. Rev. A* **92**, 022328 (2015)
34. Su, S.L., Liang, E.J., Zhang, S., Wen, J.J., Sun, L.L., Jin, Z., Zhu, A.D.: One-step implementation of the Rydberg-Rydberg-interaction gate. *Phys. Rev. A* **93**, 012306 (2016)
35. Shao, X.Q., Zheng, T.Y., Oh, C.H., Zhang, S.: One-step achievement of robust multipartite Greenberger-Horne-Zeilinger state and controlled-phase gate via Rydberg interaction. *J. Opt. Soc. Am. B* **31**, 827 (2014)

36. Shao, X.Q., Wu, J.H., Yi, X.X.: Dissipative stabilization of quantum-feedback-based multipartite entanglement with Rydberg atoms. *Phys. Rev. A* **95**, 022317 (2017)
37. Greenberger, D.M., Horne, M.A., Zeilinger, A.: Going beyond Bells theorem. in *Bells Theorem, Quantum Theory, and Conceptions of the Universe* edited by Kafatos, M. (Kluwer, Dordrecht) p.69
38. Dür, W., Vidal, G., Cirac, J.I.: Three qubits can be entangled in two inequivalent ways. *Phys. Rev. A* **62**, 062314 (2000)
39. Dür, W.: Multipartite entanglement that is robust against disposal of particles. *Phys. Rev. A* **63**, 020303 (2001)
40. Gisin, N., Massar, S.: Optimal Quantum Cloning Machines. *Phys. Rev. Lett.* **79**, 2153 (1997)
41. Cleve, R., Gottesman, D., Lo, H.K.: How to Share a Quantum Secret. *Phys. Rev. Lett.* **83**, 648 (1999)
42. Muraio, M., Jonathan, D., Plenio, M.B., Vedral, V.: Quantum telecloning and multi-particle entanglement. *Phys. Rev. A* **59**, 156 (1999)
43. Özdemir, K., Matsunaga, E., Tashima, T., Yamamoto, T., Koashi, M., Imoto, N.: An optical fusion gate for W states *New J. Phys.* **13**, 103003 (2011)
44. Ozaydin, F., Bugu, S., Yesilyurt, C., Altintas, A.A., Tame, M., Özdemir, S.K.: Fusing multiple W states simultaneously with a Fredkin gate. *Phys. Rev. A* **89**, 042311 (2014)
45. Bugu, S., Yesilyurt, C., Ozaydin, F.: Enhancing the W-state quantum-network-fusion process with a single Fredkin gate *Phys. Rev. A* **87**, 032331 (2013)
46. Han, X., Hu, S., Guo, Q., Wang, H.F., Zhu, A.D., Zhang, S.: Effective W-state fusion strategies for electronic and photonic qubits via the quantum-dot-microcavity coupled system. *Sci. Rep.* **5**, 12790 (2015)
47. Zhang, X.P., Yang, M., Ozaydin, F., Song, W., Cao, Z. L.: Generating multi-atom entangled W states via light-matter interface based fusion mechanism. *Sci. Rep.* **5**, 16245 (2015)
48. Saffman, M., Walker, T.G.: Analysis of a quantum logic device based on dipole-dipole interactions of optically trapped Rydberg atoms. *Phys. Rev. A* **72**, 022347 (2005)
49. Brion, E., Pedersen, L.H., Mølmer, K.: Implementing a neutral atom Rydberg gate without populating the Rydberg state *J. Phys. B* **40**, S159 (2007)
50. James, D.F.V., Jerke, J.: Effective Hamiltonian theory and its applications in quantum information. *Can. J. Phys.* **85**, 625 (2007)
51. Zou, X.B., Dong, Y.L., Guo, G.C.: Implementing a conditional z gate by a combination of resonant interaction and quantum interference. *Phys. Rev. A* **74**, 032325 (2006)
52. Scully, M.O., Zubairy, M.S.: *Quantum Optics*. Cambridge University Press, Cambridge (1997)